Revue Roumaine de Chimie, **2009**, *54*(6), 465–475

REDUCING THE COMPLEXITY OF COMPUTATIONAL MODELS OF NEURONS USING BIFURCATION DIAGRAMS

Sorinel A. OPRISAN

Department of Physics and Astronomy, College of Charleston, Charleston, SC 29424,
E-mail: soprisan@yahoo.com or oprisans@cofe.edu

Received December 17, 2008

We reviewed the main features of a theoretical model of dopamineric neurons able to reproduce two features observed both *in vivo* and *in vitro* experiments: 1) slow oscillatory potentials (SOP) in the presence of tetrodoxin (TTX) and tetraethyl ammonium (TEA), and 2) the square wave that can be produced by the abolition of SOP by apamin. Using bifurcation analyses, we found that not all currents and activation/inactivation functions are equally important for a coherent mathematical description. In fact, only three currents are essential: 1) the L-type calcium current, which drives both types of oscillation, 2) the small conductance (SK) potassium current, which repolarizes SOP, and 3) a slowly activating potassium current, which repolarizes the square wave. Bifurcation diagrams revealed that the model is insensitive to the kinetic details of SK current activation and that both Botzmann and Michaelis-Menten activation functions offer good descriptions of calcium-activation mechanisms.

Sorinel A. Oprisan received his B.Sc. in Physics from "Alexander Ioan Cuza" University of Iaşi, Roumania, in 1987, and his Ph.D. in Theoretical Physics from the same University in 1998. He was a faculty member of the Department of Theoretical Physics between 1990 and 1999. Between 1999 and 2005 he was a postdoctoral fellow and a research specialist in computational neuroscience in the Department of Psychology at the University of New Orleans. He also received a Mater's degree in bioinformatics from the University of New Orleans. Dr. Oprisan is currently an assistant professor of biophysics in the Department of Physics and Astronomy at the College of Charleston. His interests include computational neuroscience, particularly topologic methods of phase resetting in neural networks and computational models of dopamine neuron; applied nonlinear dynamics and chaos theory, particularly model synthesis and nonlinear time series prediction; statistical physics of complex systems, particularly Tsallis nonextensive statistics and diffusion limited aggregation mechanisms; artificial intelligence, particularly swarm intelligence and autonomous navigation, and bioinformatics, particularly protein folding and self-avoiding random walk.

INTRODUCTION

Dopaminergic neurons are involved in reward-predictive neural responses observed in a variety of cortical areas, including prefrontal cortex,[1-3] organization of goal-directed behavior[4], decision to initiate behavior with a high expectation of reward,[5] bias decision making,[6,7] learning and memory.[8] Midbrain dopamine neurons are also involved in various pathophysiologies such as Parkinson's disease,[9-11] dementia,[12,13] schizophrenia,[14,15] and drug abuse. Recent studies shed new light on the role of the increase in extracellular dopamine in the nucleus accumbens, which seems to be related to drug abuse and might impair the function of prefronto-striatal loops involved in impulse control and decision making.[16]

Since the firing pattern in these neurons determines the amount of dopamine released in the projection areas, and the burst firing pattern

releases more dopamine than a tonic one[17,18] would, an understanding of dopaminergic signaling must include an understanding of how the firing pattern is regulated. Dopamine neurons in the presence of their afferent inputs *in vivo* can exhibit one of several firing modes: silence, regular single-spike firing, irregular single-spike firing, and bursting in response to rewards or reward predicting stimuli,[19-22] but in the slice preparation, only regular single spike firing is usually observed unless pharmaceutical agents are applied. Since the dopaminergic neurons can accommodate both rapid (SOP) and slower (square wave) firing patterns, a model of dopaminergic neurons should be able to operate on a wide range of time scales.[23] We reviewed the basis for pacemaker firing and the mechanisms for transition to burst firing *in vitro*, with the goal of extrapolating these insights to the situation *in vivo*.

In a slice preparation, dopamine neurons fire in a pacemaker-like fashion, which could be abolished by the application of the L-type calcium channel blocker nifedipine in both guinea pigs[24] and rats.[25] The calcium-activated SK channel potassium current is responsible for a calcium-mediated after-hyperpolarization (AHP) after a spike.[26] The application of the calcium-activated SK potassium channel blocker apamin can also disrupt pacemaker functions by inducing burst firing in guinea pigs,[27] and in rats, apamin can covert pacemaker firing to either burst firing or irregular firing.[28]

The application of tetrodoxin (TTX) reveals spontaneous oscillatory potentials (SOP) that underlie regular pacemaker-like firing in both rats[28-30] and guinea pigs.[27,31,32] SOP are abolished in calcium-free media or by treatment with cadmium or cobalt, therefore calcium currents are essential for the depolarizing phase.[27,32-35] Furthermore, nifedipine has been shown to block SOP in both guinea pigs[27] and rats,[25] although one study found nifedipine to be ineffective,[31] Therefore, the L-type current probably plays the major role in the depolarizing phase, possibly aided to varying degrees by other calcium currents, although calcium entry via the T-type channels has also been postulated to play a role in pacemaking.[36] It was suggested both by simultaneous electrophysiological and calcium imaging experiments and *via* numeric simulations that the depolarizing phase of SOP is mediated by calcium currents and the hyperpolarizing phase is mediated by the SK current.[37,38]

Dopamine neurons can display yet another type of oscillation. Nedergaard *et al.*[27] unmasked the SOP by the application of TTX to pacemaker-like dopamine neurons in a slice preparation from a guinea pig. Then, they applied apamin and observed oscillatory plateau potentials that resembled a square wave. Ping and Shepard[28] applied the same pharmaceutical agents to dopamine neurons in a slice preparation from a rat, but in reverse order. The application of apamin induced burst firing, and the application of TTX unmasked a square wave, similar to that observed by Nedergaard *et al.,*[27]which appeared to drive the bursts. Johnson and Wu[39] (2004) duplicated these results, and were also able to convert pacemaker firing to bursting by the application of Bay K8644, which potentiates the opening of L-type channels, although the Bay K8644 induced bursting appeared qualitatively different from that induced by apamin. In some cases, the application of apamin in the absence of TTX induced irregular firing instead of bursting,[28] but if a small depolarizing current was injected, bursting could be established.[39] The bursting observed in the two studies was qualitatively similar, with slow spiking during the trough of the square wave that accelerated and diminished in amplitude during the upstroke of the square wave, and a depolarization block was observed during the plateau of the square wave.

Nifedipine blocks the square wave oscillations.[40,41] Thus, it appears that the L-type calcium channel is responsible both for the depolarizing phase of SOP and the square wave. Initially, it was suspected that a calcium-mediated process was responsible for repolarizing the plateaus as well. However, simultaneous calcium-imaging data and electrophysiological recordings during the TTX and apamin-induced square wave showed that calcium levels reached a steady state during a plateau after one second, and continued at a steady rate until plateau termination up to several seconds later.[29] Therefore a calcium-dependent mechanism is not primarily responsible for plateau repolarization.

In addition to the fast AHP mediated by the SK channel,[41] a slow, calcium-independent AHP has also been observed in dopamine cells.[36,42] Based on experimental evidences collected by Nedergaard[42] (2004), the current clearly presents features of a slowly-activating potassium channel.

MODEL

We proposed a minimal single-compartment Hodgkin-Huxley (HH)-type parallel conductance membrane model in order to capture the essential mechanisms underlying the SOP and square wave oscillations. The differential equation describing the time-dependent changes in the membrane potential is

$$C_m \frac{dV}{dt} = I_{stim} - I_{CaL} - I_{KSK} - I_{K-slow} - I_{leak}, \quad (1)$$

where C_m is the membrane capacitance[30,37,43], and I_{stim} is the external bias, I_{CaL} is the L-type calcium current, I_{KSK} is the small conductance (SK) potassium current, $I_{K\text{-}slow}$ is a slowly-activating potassium current, I_{leak} is a leak current determined by background currents for calcium, potassium and sodium, respectively. Numerical integration of the model's equations was performed on an Apple G5 workstation using an implicit fourth-order Runge-Kutta method with variable step sizes[44]. The model did not include fast sodium currents or the delayed rectifier because the model was designed to simulate only the subthreshold oscillations in the presence of TTX (blocker of fast sodium current) and TEA (blocker of potassium delayed rectifier current). All gating variables are described by first order kinetics with steady-state gating variables described by sigmoidal functions and voltage-dependent time constants described by a Gaussian relationship similar to those used by Amini *et al.*[37] We calibrated the currents using published voltage clamp data.[43,45] The input resistance of dopamine cells (n=20) was measured in the presence of apamin and TTX by using a current clamp to apply a hyperpolarized current sufficient to stop any oscillation then apply a 250 ms hyperpolarizing current pulse. The input resistance of the model measured using 250 ms hyperpolarizing pulses with an amplitude of 10 pA at -60 mV was 314 MΩ in the simulated presence of apamin ($g_{SK} = 0$) and 303 MΩ with g_{SK} set at its usual value of 4 nS, which are in the range of experimentally reported input resistances for dopamine neurons.

Experiments on a variety of dopamine neurons showed that by blocking all calcium currents with cadmium or cobalt completely silences the dopamine neurons.[31,33,34] Among other calcium currents, dopamine neurons expresses two types of low voltage activated (LVA) calcium currents, a transient (presumably T-type) and a persistent one sensitive to ω-conotoxin measured under voltage clamp conditions in the slice preparation.[43] Cordozo and Bean[46] did not usually observe LVA currents in acutely dissociated neurons from the early postnatal rat, although high-voltage activated (HVA) calcium currents were observed, and ω-agatoxin, nimodipine, and ω-conotoxin respectively blocked 35%, 30% and 20% of the HVA calcium currents. Similarly, Durante *et al.*[60] found that in slices from young rats, the same three blockers reduced the total calcium current by 34%, 27%, and 36%, with little overlap since the results were independent of the order of application.

Following Amini *et al.*,[37] only an L-type calcium current was considered in our mathematical model of the dopamine neuron. The L-type current (I_{CaL}) is described by a quick voltage-mediated activation, and a nonelectrogenic calcium pump (I_{Capump}), which was adapted from Canavier *et al.*[47] The calcium L-type current was calibrated using data from Kang and Kitai[43] (1993) for the persistent LVA calcium current that was blocked by 1 μM ω-conotoxin, but not by 10 μM nifedipine. The description of Amini *et al.*[37] also included a calcium-mediated inactivation. However, our detailed phase-space analyses showed that a calcium mediated-inactivation of L-type channels has no influence on the model's dynamics.[48] Therefore, we did not include any calcium-mediated effect in L-type current description. For the calibration of L-type calcium current, the model was held at -84 mV and clamped to -58, -48, and -38 mV (data not shown).

The equation for I_{CaL} is $I_{CaL} = g_{CaL}\, d_L\, (V - E_{Ca})$, where d_L is the time-dependent activation of L-type current given by the first order kinetics (2) with the parameters listed in Table 1.

The range of calcium excursion during the SOP was calibrated according to data that indicated a value of about 200 Nm,[29] and an approximate agreement was obtained with the calcium nullcline experimentally obtained by Wilson and Callaway.[38] Buffering was modeled simply by assuming that only a fixed fraction of the total calcium remained free in the cytosol, and that the addition of an exogenous buffer reduced this fraction. Calcium extrusion was modeled using a pump. We considered a nonelectrogenic calcium pump, therefore, the term for calcium extrusion appears only in the calcium balance. The differential equation for the rate of change of intracellular calcium is $\frac{d[Ca^{2+}]_i}{dt} = -f \frac{I_{CaL} + I_{CaB} + I_{Capump}}{2F\, vol}$, where f is a factor that takes into account the effect of calcium buffering,[38] vol is the intracellular volume of the spherical soma of radius r, and F is Faraday's constant (see Table 1). The reversal potential for the calcium currents was a constant 50 mV[30,37,43] and the calcium pump was described by equation $I_{Capump} = g_{CaP} \frac{[Ca^{2+}]_i}{[Ca^{2+}]_i + K_{Capump}}$, where g_{CaP} is the maximum current through calcium pump and

K_{Capump} is the calcium half-activation concentration for the calcium pump.

The description of the apamin-sensitive current was taken from Amini *et al.*[37] with a calcium-dependent activation function described by a Boltzmann function. We found that the exact kinetics of SK activation is not essential by comparing the results obtained with our proposed kinetics against the commonly used Michaelis-Menten kinetics[38,49,50] (data not shown). The calcium half-activation concentration value K_{SK} has been set to 190 nM in both Botzmann and Michaelis-Menten activation functions in accordance with the experimental findings, suggesting that the maximum calcium excursion in dopamine neurons during the SOP is about 200 nM.[37,51] The explicit equation for the SK current is $I_{KSK} = g_{KSK}\, p_{SK}\, (V - E_K)$, where g_{KSK} is the maximum conductance of SK channels and the calcium-mediated activation function is $p_{SK} = 1 + e^{\left([Ca^{2+}]_i - K_{SK}\right)/S_{SK}}$ (according to Amini *et al.*[37]), or $p_{SK} = \left(1 + \left(\frac{K_{SK}}{[Ca^{2+}]_i}\right)^4\right)^{-1}$ (according to Komendantov *et al.*[50]).

Slowly-activating potassium currents regulate the duration of heart action potential,[52,53] sustain spike-frequency adaptation in neurons[54] and human pancreatic β-cells,[55] and are also involved in Ca^{2+}-independent slow after-hyperpolarization of dopamine neurons,[42] Studies on these channels clearly demonstrated that the gating kinetics, as well as other properties of the different subfamilies of the ERG K^+ channels, are distinct from those of other K^+ currents.[56]

We modeled the voltage-dependent ERG current as $I_{ERG} = g_{ERG}\, d_{K\text{-}slow}\, (V - V_K)$, where the time-dependent gating variable $d_{K\text{-}slow}$ is described by the first order kinetics (2) with the steady-state activation function of the form (3), and the voltage-dependent time constant of the form (4) with the parameters listed in Table 1. The current was calibrated according to experimental data on the slow AHP, which requires more than ten seconds to activate fully, has a half decay time of about five seconds and reversed near the Nernst potential for potassium. The AHP was activated at potentials as hyperpolarized as -55 mV, and continued to activate at least until -40 mV,[42] consistent with the published half-activation voltages.[57,58]

The model also includes linear background currents for sodium (I_{NaB}), calcium (I_{CaB}) and potassium (I_{KB}).

RESULTS

Figure 1 shows typical firing patterns for the SOP (panel A) and square wave oscillations (panel B) generated using our mathematical model with the parameters reported in Table 1. The firing period of the SOP can span a firing period in the range between 200 and 600 ms, which is in good agreement with the experimentally reported data (for example, see Figure 6 in Nedergaard *et al.*[24] The application of apamin was modeled by setting $g_{KSK} = 0$ and led to square waves (or plateau potentials) similar to those observed experimentally by Ping and Shepard[59] and Nedergaard *et al.*[24] (see Figure 7 in Nedergaard *et al.*[24]). The agreement with the experimental data is quite good. The model successfully reproduces relevant physiological behavior displayed by *in vivo* and *in vitro* biological neurons. In the case of SOP, for example, where the conductance of the L-type calcium current was set to zero to simulate the replacement of external calcium by equimolar cadmium or cobalt, the oscillations were completely and suddenly abolished, and the model neuron maintained a hyperpolarized resting potential, which is consistent with experimental results.[46,60,61] I_{CaL} is also specifically blocked by nimodipine and experimental results showed a systematic cessation of spontaneous firing[24,25,61-63] consistent with the numerical results obtained with our model. In addition, the model confirms experimental observations suggesting that the small-conductance calcium-activated potassium (SK) channels present in dopamine neurons led to net inward current after the removal of Ca currents.[24] In the case of square waves, setting g_{CaL} to zero to simulate the application of nifedipine abolished the square wave oscillations and again produced a pronounced hyperpolarized steady solution (V ≈ -58 mV) at a very low calcium concentration ($[Ca^{2+}]_i \approx 20$ nM) (data not shown). Johnson and Wu[39] showed a somewhat more depolarized resting potential level in the presence of nifedipine, probably due to the contribution of calcium currents not included in our model. In addition, our numerical results are in good agreement with experimental data that showed that selectively blocking the ERG current by class III anti-arrhythmic substances, such as the

methanesulfonanilides E-4031, prolonged the duration of plateau potentials without changing the other parameters of the action potential.[56,64] Ping and Shepard[65] showed that the calcium chelator BAPTA could evoke square waves in a slice preparation in the presence of TTX but without the application of apamin. Seutin *et al.*[66,67] carried another set of experiments on dopamine neurons of neonatal rats and concluded that BAPTA chelator must act on dopamine firing pattern *via* a calcium-dependent potassium current, which was identified as the SK current. Recent experiments performed by St-Gelais *et al.*[68] suggested that the transition from plateau potential oscillations to SOP is also possible by applying neurotensin. The possible mechanism involving the increase in the firing rate due to neurotensin involves Ca^{2+}-dependent nonessential cationic conductances (possible SK currents) and the neurotensin effect is blocked by BAPTA. In addition, the experimental results of St-Gelais *et al.*[68] clearly showed that there is a significant lagtime between the increase in the firing rate induced by neurotensin and calcium elevation suggesting that Ca^{2+} elevation is necessary, yet it is not sufficient to promote firing. In our computational model, the effect of BAPTA was simulated by greatly decreasing the fraction of unbound calcium from 0.015 to 0.0004.

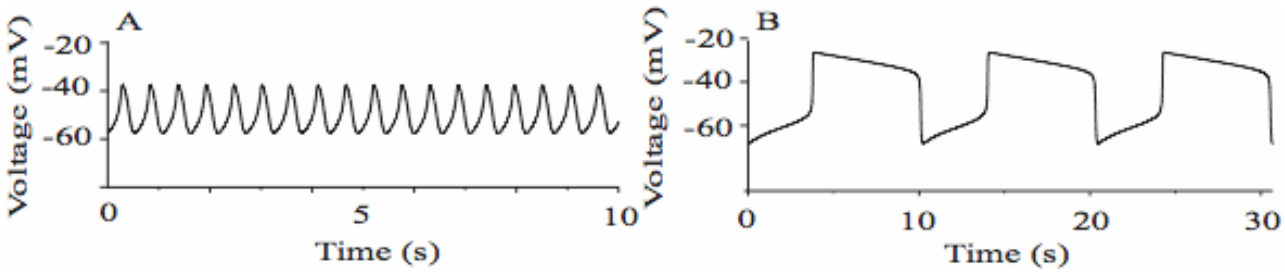

Fig. 1 – Model-generated voltage traces in the absence of sodium current (blocked by TTX) and delayed-rectifier potassium current (blocked by TEA). (A) SOP oscillations of our model have a firing period around 500 ms in good agreement with experimental measurements.[24,59] (B) Square wave oscillations were obtained from SOP by numerically integrating the model's equations with the conductance of the SK current set to zero. The intrinsic period of oscillation for the square wave is about 3300 ms and agrees with experimentally reported data.[24,59]

Table 1

Parameter values for the computational model are very similar to Amini *et al.*[37] data for sigmoidal functions. The new ERG current was calibrate according to data published by Nedergaard[42]. The values for the maximum conductance were adjusted to match electrophysioloagical data[19,20,25,30,33,43,45,46,60,80] and calcium imaging observations[29,51]

General constants F = 96500 C/mol C_m = 0.0158 pF r = 15.0 μm I_{stimul} = 0 pA f = 0.015
Background currents E_{Na} = 75.0 mV E_K = -85.0 mV E_{Ca} = 50.0 mV g_{NaB} = 0.75 nS g_{KB} = 4.25 nS g_{CaB} = 0.2 nS
Calcium L-type current g_{CaL} = 3 nS $V_{half,CaL}$ = -45.0 mV $V_{slope,CaL}$ = 7.0 mV $V_{half,\ \tau CaL}$ = -70 mV $V_{slope,\ \tau CaL}$ = 25 mV $\tau_{CaL,1}$ = 0.3 ms $\tau_{CaL,2}$ = 18 ms
Calcium pump g_{CaP} = 600 pA K_{Capump} = 500 nM
Potassium SK current g_{KSK} = 1.75 nS K_{KSK} = 190 nM
Potassium ERG current g_{ERG} = 3 nS $V_{half,\ ERGa}$ = -50.0 mV $V_{slope,\ ERGa}$ = 5.0 mV $V_{slope,\ ERGa}$ = -20.0 mV $V_{half,\ ERGi}$ = -70.0 mV $\tau_{ERGi,\ 2}$ = 0 ms $\tau_{ERGa,1}$ = 5000 ms $\tau_{ERGa,2}$ = 0 ms $\tau_{ERGi,\ 1}$ = 15 ms
Mixed afterhyperpolarization current g_H = 8 nS $V_{half,\ H}$ = -77.6 mV $V_{slope,\ H}$ = -17.3 mV $V_{half,\ \tau H}$ = -22.7 mV $V_{slope,\ \tau H}$ = 29.6 mV $\tau_{H,1}$ = 26.2 ms $\tau_{H,2}$ = 3136.0 ms

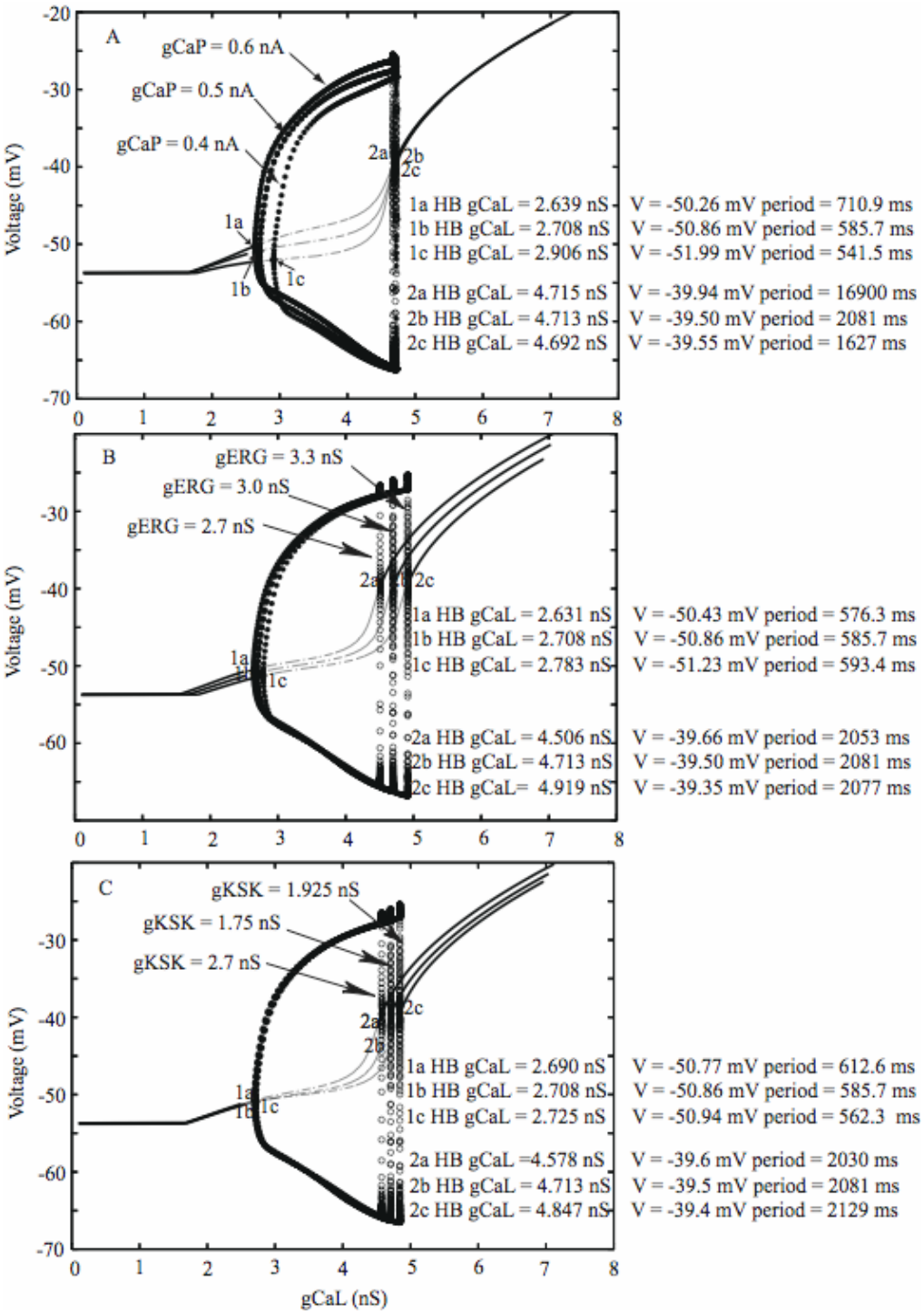

Fig. 2 – The bifurcation diagram for SOP reveals two Hopf bifurcation (HB) points. For low g_{CaL} conductance the steady hyperpolarized state becomes unstable and a stable limit cycle emerges. The period of oscillations at the onset of the limit cycle is about 500 ms and progressively increases by increasing the conductance of L-type calcium current. The influence of there other important parameters was investigated and revealed that (A) the increase of calcium pump current leads to an increase in voltage excursion and a wider range of g_{CaL} able to sustain a stable SOP, (B) an increase in the ERG conductance shifts the bifurcation points toward larger values of g_{CaL} such that the calcium influx can compensate the increase of the potassium outward current, and (C) an increase in the SK conductance shrinks the range of g_{CaL} because the calcium-dependence of SK current must be curbed by a smaller excursion in L-Type conductance in order to limit the amount of calcium inflow.

The computational models are powerful instruments because, in addition to reproducing the existing physiological data, they can predict what the outcome of a wet experiment would be if some control parameters change. There are three related computational instruments used to predict the global response of a complex system to changing parameters: 1) the frequency versus external bias (F/I) curve (see CCC2007), 2) the nullclines (CCC2007), and 3) the bifurcations diagrams. We used Bard Ermentrout's XPPAUT package[69] to extract systematic information about the structure and the stability of the firing pattern for different values of maximal current conductances. Although the model has a large number of parameters, we focused mainly on calibrating the model according to experimental data published up to this moment by tuning the maximal conductances. Qualitative descriptions of changes induced in the firing patterns due to some conductance adjustments were offered in the previous section. Quantitative information about the structure of the phase space were obtained using XPPAUT package run on an Apple G5 computers. In our bifurcation diagrams for SOP firing patterns (see Fig. 2), the maximal conductance of the L-type calcium current is the control parameter of all bifurcation diagrams due to the crucial importance of this current in SOP. We found that regardless of the values of other synaptic conductances, the model undergoes a supercritical Hopf bifurcation around g_{CaL} = 2.6 nS leading to a transition from a stable steady hyperpolarized state of $V \approx$ -50 mV to a stable limit cycle. The period of SOP at supercritical Hopf bifurcation point is around 500 ms and gradually increases to about 2000 ms. The effect of increased oscillation period suggests that a larger conductance for L-type current determines a larger calcium influx and leads to a significant contribution of a slow calcium process to the overall SOP. The amplitude of voltage oscillations is relatively small at first and slowly increases by increasing the conductance of L-type calcium current. However, for g_{CaL} above 3 nS, the amplitude of the voltage oscillations starts increasing much faster until the conductance for L-type current reaches approximately 4.5 nS and the limit cycle becomes unstable *via* another Hopf bifurcation. For larger conductance of L-type current the model neuron reaches a depolarized steady state.

Some other parameters of the model affect the generic Hopf bifurcations described above. For example, the onset of the limit cycle requires a larger conductance for L-type current if the maximal current of the calcium pump is reduced, which indicates that calcium extrusion and the L-type current are correlated in a counterintuitive way due to the presence of the SK current (see Fig. 2A). In addition, a larger maximal current for the calcium pump leads to a slight increase in the depolarization level of voltage oscillations, which is suggest a larger and larger influence of calcium-mediated small-conductance potassium current.

Any increase in the conductance of the ERG current slightly shifts both Hopf bifurcation points toward larger conductances for the L-type current (see Fig. 2B) which reflects the fact that the outward ERG current is compensated by an appropriate inward contribution from the L-type current.

The increase in the conductance of SK current shrinks the range of L-type conductance that leads to periodic and stable oscillations. Increasing the conductance for the SK current tends to shift the position of the second Hopf bifurcation point toward smaller conductance for the L-type current to compensate the increased outward potassium current (see Fig. 2C).

We focus our investigation of the bifurcation diagrams for square waves only on L-type calcium current and the ERG current because these two currents are driving the model neuron (see Fig. 3). The bifurcation structure looks similar to SOP having two major Hopf bifurcation (HB) points. One significant difference is that the range of L-type calcium conductance is much narrower due to a tighter need for a balance between fast activating L-type current and much slower ERG current (compare Fig. 2B versus Fig. 3A).

At the same time, by magnifying the two small portions of the bifurcation diagram shown in Fig. 3A located around the left Hopf bifurcations (Fig. 3B) and right Hopf bifurcation (Fig. 3C), we can observed that there exists a finer bifurcation structure. For example, at the onset of the HP (Fig. 3B), the steady hyperpolarized state coexists with a stable (filled circles) small amplitude periodic oscillation. These are subthreshold oscillations determined by the fact that the conductance of the L-type current is too small to determine a significant influx of calcium in order to trigger a significant ERG current. It is also possible to obtain large amplitude oscillations even at smaller conductance for L-type current by reducing the calcium pump maximal current (bifurcation diagrams not shown). By increasing the conductance of L-type current, the small amplitude limit cycle becomes unstable (open circles) and a period doubling (PD) bifurcation occurs. At the other end of the bifurcation diagram, the steady depolarized state becomes unstable via a Hopf bifurcation (Fig. 3C). At first, the amplitude of oscillations is small, but after it reaches a limit point (LP), the peak-to-peak amplitude reaches its maximum.

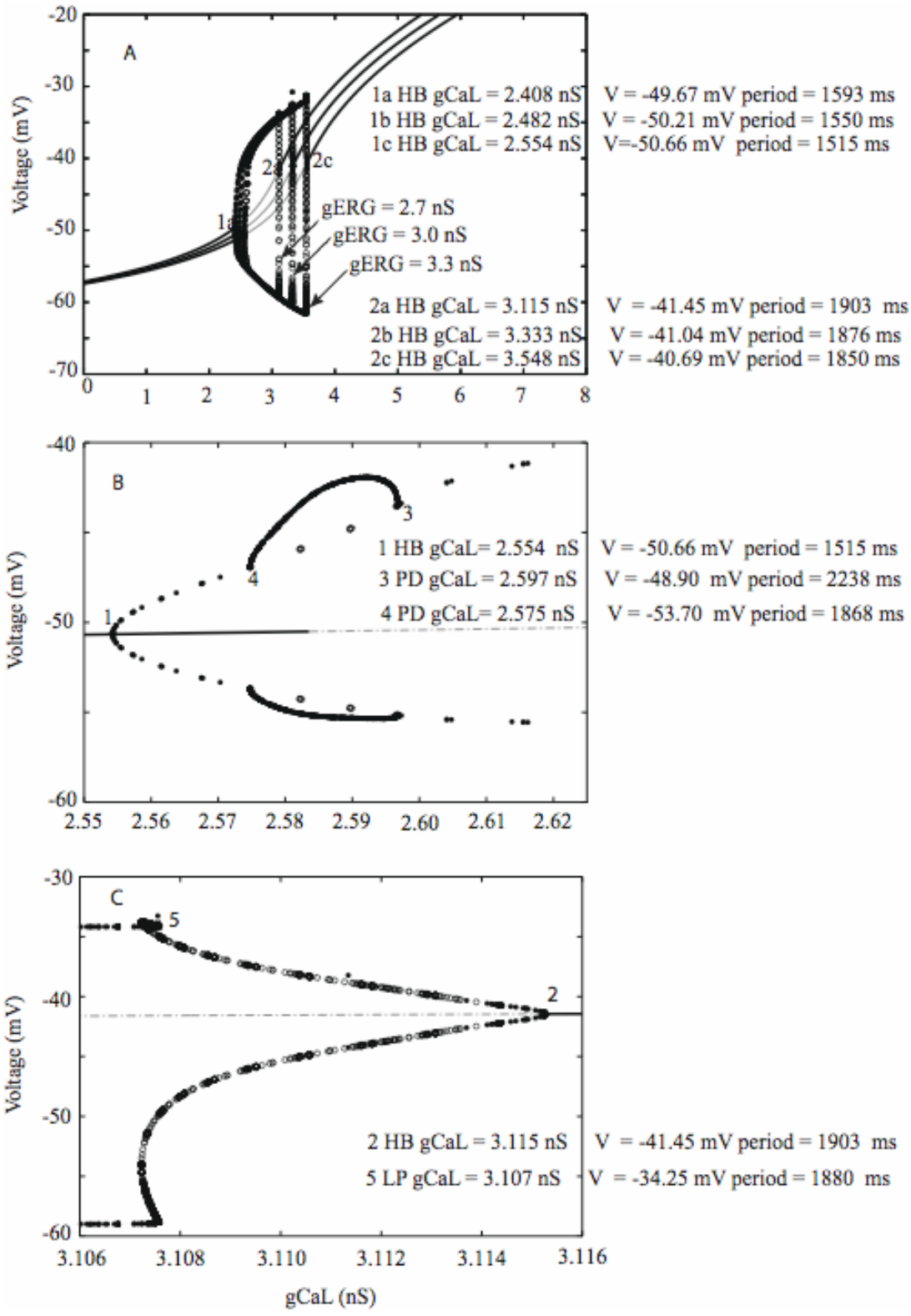

Fig. 3 – The bifurcation diagram for square-waves has two Hopf bifurcation points and a reach structure at a finer scale. (A) The major current involved in square-wave generation are L-type calcium current and ERG current. Increasing the conductance of the ERG current leads to an increase in the amplitude of the voltage oscillations. (B) The subthreshold oscillations occur near the HB point. By increasing the conductance of the L-type current, a period doubling (PD) bifurcation occurs. (C) Small amplitude oscillations also occur near the second HB point at the crossing between the steady depolarization and the limit cycle oscillations.

CONCLUSIONS

Little is known about the mechanism of calcium removal in dopamine neurons, although we presume that the calcium pump rather than an exchanger is primarily responsible.[70] One piece of evidence argues against completely electrogenic calcium removal, in which the removal of a calcium ion from the cell results in the net removal of two positive charges from the cell. If this were the case, in a steady state, not only would the rates of calcium influx and efflux be balanced, but so would the rates of influx and efflux. If that were the case, no persistent inward calcium current could be observed after the calcium concentration at a particular voltage equilibrated, which is contrary to experimental observations.[30,38] Some studies have shown that protons can enter the cell as calcium is pumped out, reducing the electrogenicity of the pump.[71] An early study using sharp electrodes[65] indicated that the plateaus evoked by intracellular chelation of calcium lengthened the plateaus compared to those observed in apamin, which might indicate that another calcium mediated process also contributes to plateau repolarization. This study suggests that blocking the calcium pump with vanadate would not affect the square wave.

An interesting possibility is that the effect of ω-Aga-IVA on peacemaking, which requires a P/Q-type calcium current, is indirectly mediated by the calcium pump. Although recent experiments on peacemaking cells in the cardiac senatorial node suggested a major role for depolarizing current produced by the Na-Ca exchanger,[72] it might be possible to adjust the electrogeneity of the calcium pump in order to attain a similar result. It is clear that dopamine neuron peacemaking involves a significant infusion of calcium. The mechanisms for removal of this large calcium entry remain to be characterized in more detail and could involve both an electrogenic calcium pump and the Na-Ca exchanger.

In this study, we simulated square wave oscillations that include a depolarized plateau in the presence of apamin and TTX. In the presence of apamin only, burst firing is observed instead. The bursts are unusual because the spiking occurs during the hyperpolarized phase, then a high frequency burst occurs on the upstroke of the plateau, and usually a depolarization block occurs during the final portion of the plateau. Recent experimental results[73] have shown that the specific ERG blocker[74,75] E 4031 does indeed elongate the plateau in the presence of TTX and apamin just as predicted by our computational model. Thus, we hypothesize that the ERG current helps relieve a depolarization block, and may relieve it *in vivo* as well.

When dopamine neurons are depolarized excessively, such as during the plateaus of apamin-induced burst firing, inactivation of the fast sodium current cannot be removed between spikes and spiking ceases until the neuron is sufficiently hyperpolarized to relieve this inactivation. High concentrations of NMDA have been shown to induce a depolarization block both *in vivo* and *in vitro,*[76] and L-glutamate has also been shown to be capable of inducing a depolarization block *in vitro,*[77] therefore a depolarization block may also occur *in vivo* under conditions of excessive glutamatergic stimulation.

A role for a depolarization block of midbrain dopamine neurons has been postulated in the treatment of schizophrenia with antipsychotic drugs. Drugs such as trifluoperazine, a phenothiazine, are effective in treating schizophrenia since they can block dopamine receptors in the central nervous system.[75,76]

However, since the synaptic block occurs very rapidly yet it takes weeks to achieve therapeutic efficacy, it seems that the homeostatic response of the brain to dopamine receptor block may actually be responsible for the therapeutic effects of antipsychotics.[80] A delayed increase in the depolarization-induced block of the electrical activity of midbrain dopamine cells in animals chronically treated with antipsychotics has been observed with a time course that may correlate with that of the therapeutic response.[80] The following explanation has been proposed for the delayed increase in depolarization block: dopamine acts both on autoreceptors that inhibit the dopamine neurons and at the postsynaptic terminals on the targets of the axons on dopamine cells.

The anti-psychotic haloperidol acts quickly to block autoreceptors, causing a disinhibition of dopamine cell firing, while simultaneously blocking the effect of dopamine release onto the target neurons.[81] Grace *et al.*[80,82] have proposed that the slow time course of therapeutic action correlates with the feedback from the target neurons attempting to keep the level of activation of the postsynaptic dopamine receptors in a target range, by increasing net excitatory input to the dopamine neurons to compensate for dopamine receptor blockage. However, the increased net excitation drives the neurons increasingly into the depolarization blockage, which further reduces the

stimulation of postsynaptic receptors due to the cessation of spiking activity.

It is known for a long time that some of antipsychotic drugs in therapeutic doses have been associated with sudden death[83] and it is believed that their side effect is due to the simultaneous blockage of ERG cardiac channels.[80,84,85]

In this study, we show that the ERG current likely contributes to relief from depolarization block in a nonphysiological setting, under conditions of apamin-induced block of the SK channel in a slice preparation. It is also possible that the ERG acts to relieve depolarization blockage *in vivo*, both under normal physiological conditions and in persons taking antipsychotics. The postulated role of depolarization block in the action of antipsychotic drugs used to treat schizophrenia combined with our suggestion that the ERG channel may also relieve depolarization blockage under physiological conditions *in vivo* implies that antipsychotics may derive some of their therapeutic benefits from their effects on the neural ERG channel.

In addition, the ERG channels can be selectively blocked not only by class III antiarrhythmic substances such as the methanesulfonanilides E-4031 and WAY-123,398, but also by some widely used neuroleptics, such as haloperidol and histamine-receptor antagonists like terfenadine. These pharmacological effects explain the serious cardiac side effects of these widely used therapeutic agents.

At the same time, other experimental studies suggested that phenothiazine-induced arrhythmia and death were not produced via the central nervous system.[86] It is possible that the ERG channels expressed in the central nervous system have a slightly different biochemical structure compared to cardiac ERG channels and the two channels could be targeted by fine-tuned drugs.[87]

Acknoledgments: This work was supported by a Research and Development grant from the College of Charleston to S. Oprisan.

REFERENCES

1. K.I. Amemori and T. Sawaguchi, *Cerebral Cortex*, **2006**, *16*, 1002–1015.
2. D.J. Barraclough, M.L. Conroy, and D. Lee, *Nature Neurosci.*, **2004**, *7*, 404–410.
3. K. Matsumoto, W. Suzuki, and K. Tanaka, *Science*, **2003**, *301*, 229–232.
4. B.W. Ballein and A. Dickinson, *Neuropharmacology*, **1998**, *37*, 407–419.
5. K. Matsumoto and K. Tanaka, *Curr. Opin. Neurobiol.*, **2004**, *14*, 178–185.
6. R.J. Dolan, *Science*, **2002**, *298*, 1191–1194.
7. J.I. Gold and M.N. Shadlen, *Neuron*, **2002**, *36*, 299–308.
8. M. El-Ghundi, B.F.O'Dowd, and S.R. George, *Rev. Neurosci.*, **2007**, *18*, 37–66.
9. H. Bernheimer, W. Birkmayer, O. Hornykiewicz, K. Jellinger, and F. Seitelberger, *J. Neurol. Sci.*, **1973**, *20*, 415–455.
10. W.M. Caudle, J.R. Richardson, M.Z. Wang, T.N. Taylor, T.S. Guillot, A.L. McCormack, R.E. Colebrooke, D.A.D. Monte, P.C. Emson, and G.W. Miller, *J. Neurosci.*, **2007**, *27*, 8138–8148.
11. X.Y. Chen, J.Li, W. Q. Qi, and S.H. Shen, *Histol. Histopathol.*, **2007**, *22*, 1085–1090.
12. R. Lakshmana, S. Sundram, and F. Cairns, *Psychogeriatrics*, **2006**, *6*, 31–41.
13. F. Sedaghat, A. Gotzamani-Psarrakou, E. Dedousi, M. Arnaoutoglou, K. Psarrakos, I. Koob, G. F., H.T. Le, and I. Creese, *Neurosci. Letters*, **1987**, *79*, 315–320.
14. E.M. Meisenzahl, G.J. Schmitt, J. Scheuerecker, and H.J. Moller, *Int. Rev. Psychiatry.*, **2007**, *19*, 337–345.
15. D.R. Weinberger, *Arch. Gen. Psychiatry*, **1987**, *44*, 660–669.
16. G.D. Chiara, and V. Bassareo, *Current Opinion in Pharmacology*, **2007**, *7*, 69–76.
17. J. Chergui, G.G. Nomikos, J.M. Mathe, F. Gonon, and T.H. Svensson, *Neuroscience*, **1996**, *72*, 141–156.
18. F.G. Gonon, *Neuroscience*, **1988**, *24*, 19–28.
19. A.A. Grace, and B.S. Bunney, *J. Neurosci.*, **1984**, *4*, 2866–2876.
20. A. Grace, and B. Bunney, *J. Neurosci.*, **1984**, *4*, 2877–2890.
21. B.I. Hyland, J.N. Reynolds, J. Hay, C.G. Perk, and R. Miller, *Neuroscience*, **2002**, *114*, 475–492.
22. W. Schultz, *J. Neurophysiol.*, **1998**, *80*, 1–27.
23. M.L.A.V. Heien, A.S. Khan, J.L. Ariansen, J.F. Cheer, P.E.M. Phillips, K.M. Wassum, and R.M. Wightman, *Proceedings of the National Academy of Sciences of the USA*, **2005**, *102*, 10023–10028.
24. S. Nedergaard, J.A. Flatman, and I. Engberg, *J. Physiol.*, **1993**, *466*, 727–747.
25. N.B. Mercuri, A. Bonci, P. Calabresi, F. Stratta, A. Stefani, and G. Bernardi, *Br. J. Pharmacol.*, **1994**, *113*, 831–838.
26. P.D. Shepard, and B.S. Bunney, *Exp. Brain. Res.*, **1991**, *86*, 141–150.
27. S. Nedergaard, and S.A. Greenfiels, *Neuroscience*, **1992**, *48*, 423–437.
28. H.X. Ping, and P.D. Shepard, *Neuroreport*, **1996**, *7*, 809–814.
29. J.C. Callaway, C.J. Wilson, and P.D. Shepard, *Proc. Soc. Neurosci.*, **2000**, *30*, 556.3.
30. Y. Kang, and S. Kitai, *Neurosci. Research*, **1993**, *18*, 195–207.
31. K. Fujimura, and Y. Matsuda, *Neurosci. Letters*, **1989**, *10*, 453–457.
32. W.H. Yung, M.A. Hausser, and J.J.B. Jack, *J. Physiol.*, **1991**, *426*, 643–667.
33. A.A. Grace, and S.-P. Onn, *J. Neurosci.*, **1989**, *9*, 3463–3481.
34. N.C. Harris, C. Webb, and S.A. Greenfield, *Neuroscience*, **1989**, *31*, 355–362.
35. T. Kita, H. Kita, and S.T. Kitai, *Brain Research*, **1986**, *372*, 21–30.
36. J. Wolfart, and J. Roeper, *J. Neurosci.*, **2002**, *22*, 3404–3413.
37. B .Amini, J.W.C. Jr., and C.C. Canavier, *J. Neurophysiol.*, **1999**, *82*, 2249–2261.
38. C.J. Wilson, and J.C. Callaway, *J. Neurophysiol.*, **2000**, *83*, 3084–3100.

39. S.W. Johnson, and Y.N. Wu, *Brain Research*, **2004**, *1019*, 293–296.
40. S. Johnson, V. Seutin, and R.A. North, *Science*, **1992**, *258*, 665–667.
41. P.D. Shepard, and D. Stump, *Brain Research*, **1999**, *877*, 104–109.
42. S. Nedergaard, *Neuroscience*, **2004**, *125*, 841–852.
43. Y. Kang, and S. Kitai, *Neurosci. Research*, **1993**, *18*, 209–221.
44. E. Hairer, and G. Warner, "Solving Ordinary Differential Equations. II. Stiff and Differential-Algebraic Problems", Springer-Verlag, New York, 1990.
45. N.B. Mercuri, A. Bonci, P. Calabresi, A. Stefani, and G. Bernardi, *Eur. J. Neurosci.*, **1995**, *7*, 462–469.
46. D.L. Cordozo, and B.P. Bean, *J. Neurophysiol.*, **1995**, *743*, 1137–1148.
47. C.C. Canavier, J.W.C. Jr., and J.H. Byrne, *J. Neurophysiol.*, **1991**, *66*, 2107–2124.
48. S.A. Oprisan, and C.C. Canavier, *Neurocomputing*, **2006**, *69*, 1030–1034.
49. M. Kohler, B. Hirschberg, C.T. Bond, J.M. Kinzie, N.V. Marrion, J. Maylie, and J.P. Adelman, *Science*, **1996**, *273*, 1709–1714.
50. A.O. Komendantov, O.G. Komendantova, S.W. Johnson, and C.C. Canavier, *J. Neurophysiol.*, **2004**, *91*, 346–357.
51. J.C. Callaway, and C.J. Wilson, *Proc. Soc. Neurosci.*, **1997**, *23*, 1278.
52. M.C. Sanguinetti, C. Jiang, M.E. Curran, and M.T. Keating, *Cell*, **1995**, *81*, 299–307.
53. M. Sanguinetti, and N. Jurkiewicz, *J. Gen. Physiol.*, **1990**, *96*, 195–215.
54. N .Chiesa, B. Rosati, A. Arcangeli, M. Olivotto, and E. Wanke, *J. Physiol. (London)*, **1997**, *501*, 313–318.
55. B. Rosati, P. Marchetti, O. Crociani, M. Lecchi, R. Lupi, A. Arcangeli, M. Olivotto, and E. Wanke, *FASEB*, **2000**, *14*, 2601–2610.
56. J.R. Schwarz, and C.K. Bauer, *News Physiol. Sci.*, **1999**, *14*, 135–142.
57. M.J. Saganich, E. Machado, and B. Rudy, *J. Neurosci.*, **2001**, *21*, 4609–4624.
58. R. Schonherr, K. Lober, and S.H. Heinemann, *EMBO*, **2000**, *19*, 3263–3271.
59. H.X. Ping, and P.D. Shepard, *J. Neurophysiol.*, **1999**, *81*, 977–984.
60. P. Durante, C.G. Cardenas, J.A. Whittaker, S.T. Kitai, and R.S. Scroggs, *J. Neurophysiol.*, **2004**, *91*, 1450–1454.
61. M. Puopolo, E. Raviola, and B.P. Bean, *J. Neurosci.*, **2007**, *27*, 645–656.
62. A. Pignatelli, K. Kobayashi, H. Okano, and O. Belluzzi, *J. Physiol. (London)*, **2005**, *564*, 501–514.
63. M .Puopolo, B. Bean, and E. Raviola, *J. Neurophysiol.*, **2005**, *94*, 3618–3627.
64. W. Spinelli, I.F. Moubarak, R.W. Parsons, and T.J. Colatsky, *Cardiovasc. Res.*, **1993**, *27*, 1580–1591.
65. H. Ping, and P. Shepard, *Proc. Soc. Neurosci.*, **1997**, *23*, 1211.
66. V. Seutin, L. Massotte, J. Scuvee-Moreau, and A. Dresse, *J. Neurophysiol.*, **1998**, *80*, 3361–3364.
67. V. Seutin, F. Mkahli, L. Massotte, and A. Dresse, *J. Neurophysiol.*, **2000**, *83*, 192–197.
68. F .St-Gelais, M. Legault, M.J. Bourque, P.P. Rompre, and L.E. Trudeau, *J. Neurosci.*, **2004**, *24*, 2566–2574.
69. B. Ermentrout, "Simulating, Analyzing, and Animating Dynamical Systems: A Guide to XPPAUT for Researchers and Students". Soc. for Industr. & Appl. Math, Philadelphia, 2002.
70. J.M. Salvador, G. Inesi, J.L. Rigaud, and A.M. Mata, *J. Biol. Chem.*, **1998**, *273*, 18230–18234.
71. N. Wanaverbecq, S.J. Marsh, M. Al-Qatari, and D.A. Brown, *J. Physiol.*, **2003**, *550*, 83–101.
72. L. Sanders, S. Rakovic, M. Lowe, P.A. Mattick, and D.A. Terrar, *J. Physiol. (London)*, **2006**, *571*, 639–649.
73. S.A. Oprisan, P.D. Shepard, and C.C. Canavier, *Proc. Soc. Neurosci.*, **2005**, *97*, 100.
74. P.S. Spector, M.E. Curran, M.T. Keating, and M.C. Sanguinetti, *Circ. Res.*, **1996**, *78*, 499–503.
75. F. Weinsberg, C.K. Bauer, and J.R. Schwarz, *Pflugers Arch.*, **1997**, *434*,1–10.
76. X. Wang, P. Zhong, Z. Gu, and Z. Yan, *J. Neurosci.*, **2003**, *23*, 9852–9861.
77. T. Wang, and E.D. French, *Brain Research*, *1993*, *627*, 229–306.
78. S.-Y. Choi, Y.-S. Koh, and S.-H. Jo, *J. Pharmacol. Exp. Therap.*, **2005**, *313*, 888–895.
79. P. Seeman, *Pharmacol. Rev.*, **1980**, *32*, 229–313.
80. A.A. Grace, B.S. Bunney, H. Moore, and C.L. Todd, *Trends in Neuroscience*, **1997**, *20*, 31–37.
81. H .Suessbrich, R. Schonherr, S.H. Heinemann, B. Attali, F. Lang, and A.E. Busch, *Br. J. Pharmacol.*, **1997**, *120*, 968–974.
82. A.A. Grace, *Addiction*, **2000**, *95*, S119–128.
83. H.G. Kelly, J.E. Fay, and S.G. Laverty, *Can. Med. Assoc.*, **1963**, *89*, 546–554.
84. P.G. Strange, *Pharmacol. Rev.*, **2001**, *53*, 119–133.
85. M .Taglialatela, P. Castaldo, A. Pannaccione, G. Giorgio, and L. Annunziato, *Biochem. Pharmacol.*, **1998**, *55*,1741–1746.
86. L.J. Lipka, C.M. Lathers, and J. Roberts, *J. Clin. Pharmacol.*, **1988**, *28*, 968–983.
87. C.C. Carmen, S.A. Oprisan, J. Callaway, H. Ji, and P.D. Shepard, *J Neurophysiol*, **2007**, *98*, 3006-3022.